IPCC's Twentieth-Century Climate Simulations: Varied Representations of North American Hydroclimate Variability

ALFREDO RUIZ-BARRADAS

Department of Atmospheric and Oceanic Science, University of Maryland, College Park, College Park, Maryland

SUMANT NIGAM

Department of Atmospheric and Oceanic Science, and Earth System Science Interdisciplinary Center, University of Maryland, College Park, College Park, Maryland

(Manuscript received 23 May 2005, in final form 23 November 2005)

ABSTRACT

The annual cycle of precipitation and the interannual variability of the North American hydroclimate during summer months are analyzed in coupled simulations of the twentieth-century climate. The state-of-the-art general circulation models, participating in the Fourth Assessment Report for the Intergovernmental Panel on Climate Change (IPCC), included in the present study are the U.S. Community Climate System Model version 3 (CCSM3), the Parallel Climate Model (PCM), the Goddard Institute for Space Studies model version EH (GISS-EH), and the Geophysical Fluid Dynamics Laboratory Coupled Model version 2.1 (GFDL-CM2.1); the Met Office's Third Hadley Centre Coupled Ocean–Atmosphere GCM (UKMO-HadCM3); and the Japanese Model for Interdisciplinary Research on Climate version 3.2 [MIROC3.2(hires)]. Datasets with proven high quality such as NCEP's North American Regional Reanalysis (NARR), and the Climate Prediction Center (CPC) U.S.–Mexico precipitation analysis are used as targets for simulations.

Climatological precipitation is not easily simulated. While models capture winter precipitation very well over the U.S. northwest, they encounter failure over the U.S. southeast in the same season. Summer precipitation over the central United States and Mexico is also a great challenge for models, particularly the timing. In general the UKMO-HadCM3 is closest to the observations.

The models' potential in simulating interannual hydroclimate variability over North America during the warm season is varied and limited to the central United States. Models like PCM, and in particular UKMO-HadCM3, exhibit reasonably well the observed distribution and relative importance of remote and local contributions to precipitation variability over the region (i.e., convergence of remote moisture fluxes dominate over local evapotranspiration). However, in models like CCSM3 and GFDL-CM2.1 local contributions dominate over remote ones, in contrast with warm-season observations. In the other extreme are models like GISS-EH and MIROC3.2(hires) that prioritize the remote influence of moisture fluxes and neglect the local influence of land surface processes to the regional precipitation variability.

1. Introduction

Extreme weather and climate events have profound impact on the societies and environment of the regions affected. Events like Europe's major heat wave during the summer of 2003, the above-average Atlantic hurricane activity in both 2003 and 2004, the first hurricane ever in the South Atlantic in 2004, the above-normal rain and crops in the Sahel region during the 2003–04 cycle, and the persistent drought condition over western United States (e.g., see the extreme weather and climate events Web site from the National Climate Data Center online at http://lwf.ncdc.noaa.gov/oa/climate/severeweather/extremes.html), are easily deemed as evidence of the presence of global warming by the media and population.

Attending to the heterogeneity of the distribution of the climate controls over the planet there is no basis to expect that, under the scenario of a global climate change, extreme events will be of the same type everywhere in the world. Thus, it is important to understand the regional climates before ascertaining the effects of

Corresponding author address: Alfredo Ruiz-Barradas, Department of Atmospheric and Oceanic Science, University of Maryland, College Park, 3405 Computer and Space Sciences Bldg., College Park, MD 20742-2425.
E-mail: alfredo@atmos.umd.edu

global climate change over specific regions. A clear understanding of the current and future climate can only be achieved by analyzing observed data and conducting modeling studies.

Interest in regional climate change, specially hydroclimate, is intense due to the increasing societal needs for sustainable water supply, management of water resources, and mitigation/prevention of hazardous hydroclimate episodes. Hence, the economic and social value of regional hydroclimate predictions is unquestionable. The scientific value is also enormous, especially if the region is densely observed, for it can then provide an opportunity for model validation. A region of great hydroclimate interest is North America, where water resources are recharged during winter and early spring months, and largely depleted during summer months.

The authors have recently concluded an analysis of Great Plains hydroclimate variability focusing on the anomalous atmospheric water balance in the warm-season months in observations, reanalyses, and state-of-the-art atmospheric simulations (Ruiz-Barradas and Nigam 2005, 2006). The structure of precipitation and the role of local and remote water sources—evaporation and moisture fluxes, respectively—in producing precipitation variability were examined. The main finding is the dominance of remote water sources over local ones in nature (as suggested for reanalyses data and observed and observationally constrained data) and quite the opposite in simulations.

In the present study, largely motivated and based on the authors' previous research, the diagnostic analysis of hydroclimate variability during the warm season is carried out on coupled simulations. Specifically, the realism of North American hydroclimate variability is evaluated in the coupled simulations of the current climate. At issue are the relative contributions of the atmospheric water balance terms in producing precipitation variability over the central United States. The models in the present analysis are state-of-the-art coupled general circulation models (GCMs) participating in the Fourth Assessment Report of the Intergovernmental Panel on Climate Change (IPCC).

Models analyzed include four U.S. models, a British model, and a Japanese model. The U.S. models are the Community Climate System Model version 3 (CCSM3), and the Parallel Climate Model (PCM) from the National Center for Atmospheric Research (NCAR); the Geophysical Fluid Dynamics Laboratory Coupled Model version 2.1 (GFDL-CM2.1) from the National Oceanic and Atmospheric Administration (NOAA); and the Goddard Institute for Space Studies model version EH (GISS-EH) from the National Aeronautics and Space Administration (NASA). The United Kingdom model is the Met Office's Third Hadley Centre Coupled Ocean–Atmosphere GCM (UKMO-HadCM3). The Japanese model is the high-resolution Model for Interdisciplinary Research on Climate version 3.2 [MIROC3.2(hires)] from the Center for Climate System Research at the University of Tokyo (CCSR), the National Institute of Environmental Studies (NIES), and the Frontier Research System for Global Change (FRSGC).

The datasets used in hydroclimate validation are described in section 2. The annual cycle of precipitation is briefly described in section 3. The Great Plains precipitation variability is discussed in section 4; in addition, the frequency of anomalous events is compared. The accompanying spatial patterns of precipitation, stationary moisture fluxes, and evaporation linked to precipitation variability over the region are the focus in section 5; the relative contributions from moisture flux convergence and evaporation to precipitation variability are also compared in this section. The validity of the results is further investigated in section 6 via autocorrelation analysis. Concluding remarks are presented in section 7.

2. Datasets

The North American Regional Reanalysis (NARR) dataset, from the National Centers for Environmental Predictions (NCEP), is used in the models' assessment. The studies by Ruiz-Barradas and Nigam (2005, 2006) set up the basis of the methodology followed, as well as the target dataset used for the present analysis. The regional reanalysis is a long-term, consistent, data assimilation–based, climate data suite for North America (see online at http://wwwt.emc.ncep.noaa.gov/mmb/rreanl/; Mesinger et al. 2004). The regional reanalysis is produced at high spatial and temporal resolutions (32 km, 45 layer, 3 hourly) and spans a period of 25 yr from October 1978 to December 2003; it is based on the April 2003 frozen version of NCEP's mesoscale Eta forecast model and its data assimilation system (EDAS). NARR assimilates precipitation unlike the global reanalyses from NCEP (Kalnay et al. 1996) and the 40-yr European Centre for Medium-Range Weather Forecasts (ECMWF) Re-Analysis (ERA-40; see online at http://www.ecmwf.int/products/data/archive/descriptions/e4/). The assimilation is, in fact, successful with downstream effects, including two-way interaction between precipitation and the improved land surface model (e.g., Mitchell et al. 2004); this implies an observationally constrained evaporation field that is in line with some other observationally constrained products.

Evaluation of the NARR dataset was already done in Ruiz-Barradas and Nigam (2006), and Nigam and Ruiz-

Barradas (2006) and expands on the consistency of the dataset to be used as target of the simulations, especially in the context of interannual variability over North America. For purposes of the present examination, the analysis on NARR is repeated on the same resolution used in the simulations, that is, an R30 (96 × 80) Gaussian grid for the 1979–98 period.

The regional reanalysis is limited in time so an ancillary, longer precipitation dataset is also used. The dataset of choice for U.S.–Mexico precipitation is the NOAA/Climate Prediction Center (CPC) retrospective analysis of daily station data (see online at http://www.cpc.ncep.noaa.gov/products/precip/realtime/retro.shtml; hereafter referred to as the U.S.–Mexico dataset), which was extensively used for validation in Ruiz-Barradas and Nigam (2005, 2006).

As mentioned earlier, simulations from six models are assessed. However, three other models[1] were analyzed but not included due to space limitations and redundancy of the results in the context of the present paper. The six models, CCSM3 (published in the 1 June special issue of the *Journal of Climate*), GFDL-CM2.1 (Delworth et al. 2006), GISS-EH (Schmidt et al. 2006), PCM (Meehl et al. 2004), UKMO-HadCM3 (Gordon et al. 2000; Pope et al. 2000), MIROC3.2(hires) (Hasumi and Emori 2004), are representatives of major climate research centers in the world.

Historical simulations of the twentieth-century climate are analyzed. Those are simulations where coupled GCMs are being forced by observed solar irradiance, volcanic and anthropogenic aerosols, and atmospheric concentrations of ozone, carbon dioxide, and other well-mixed greenhouse gases (http://www-pcmdi.llnl.gov/ipcc/climate_forcing.php).[2] In general, the model simulations are century long starting in the second half of the 1800s and ending in 1999.

The analysis period will focus on the more recent 48 yr (1951–98) of the century-long coupled simulations. The warm-season months of June–July–August (JJA) are the focal point of the analysis. Interannual variability is analyzed using monthly anomalies, calculated with respect to the 1951–98 monthly climatology. Simulated fields were homogenized for all models extrapolating them to an R30 (96x80) Gaussian grid. Stationary horizontal moisture fluxes are calculated as in Ruiz-Barradas and Nigam (2005), by computing the mass-weighted vertical integral from the surface to 300 hPa in both regional reanalysis and simulations.[3] Statistical significance of correlations and regressions are evaluated using a Student's *t* test at the 0.05 level.

3. Precipitation annual cycle

The annual march of monthly precipitation is analyzed here through harmonic analysis of the 12-month climatology.[4] The interest is on the annual cycle so the analysis is focused on the first harmonic as in Nigam and Ruiz-Barradas (2006). Attention is paid to the amplitude and timing of the annual cycle in the different datasets over the continent; mean annual precipitation (i.e., mean of the 12-month climatology) is also compared as background to the harmonic analysis plots (Fig. 1). Amplitude of the annual cycle is indicated by the length of the vector while phases are indicated by the orientation of the arrows according to the inserted scaling vector; thus, an arrow pointing to the south indicates a maximum on 1 January, one pointing to the west means a maximum on 1 April, one pointing toward the north indicates a maximum on 1 July, and one pointing to the east means a maximum on 1 October.

In general the amplitude of the observed annual cycle, and very well represented here by NARR, diminishes and occurs earlier in the summer months from tropical Mexico to the central United States (arrows in Fig. 1a). Notable observed features include the following: the maximum over the northwestern United States in January, the maximum over the central United States during June–July, a weak maximum over the southern states during the late winter/early spring months, and weak seasonal variability over the Atlantic states. Additionally, in August there are maxima over northwestern Mexico as well as over central and southern Mexico; those amplitudes diminish from south to north. The structure of the mean annual precipitation in NARR (contours in Fig. 1a) is given by seasonal contributions in both the northwestern and southern United States during winter, and the central United States and Mexico during summer, just as in observations (see Nigam and Ruiz-Barradas 2006 for further details).

[1] The GFDL-CM2.0: GFDL's coupled model version 2.0, GISS-ER: GISS's *ER* coupled model, and GISS-AOM: GISS's 4° × 3° coupled model.

[2] It is not clear how many models used historical land-use change as a forcing for their twentieth-century simulations. While the GFDL models (CM2.0 and CM2.1) included it, CCSM3 did not.

[3] UKMO-HadCM3 does not provide data at the 925-hPa standard level but does it at the 950-hPa level instead.

[4] Climatologies are calculated for the common 1979–98 period for both NARR and simulations. Minimum, and negligible, differences appear if the 1951–98 period is used for the simulations.

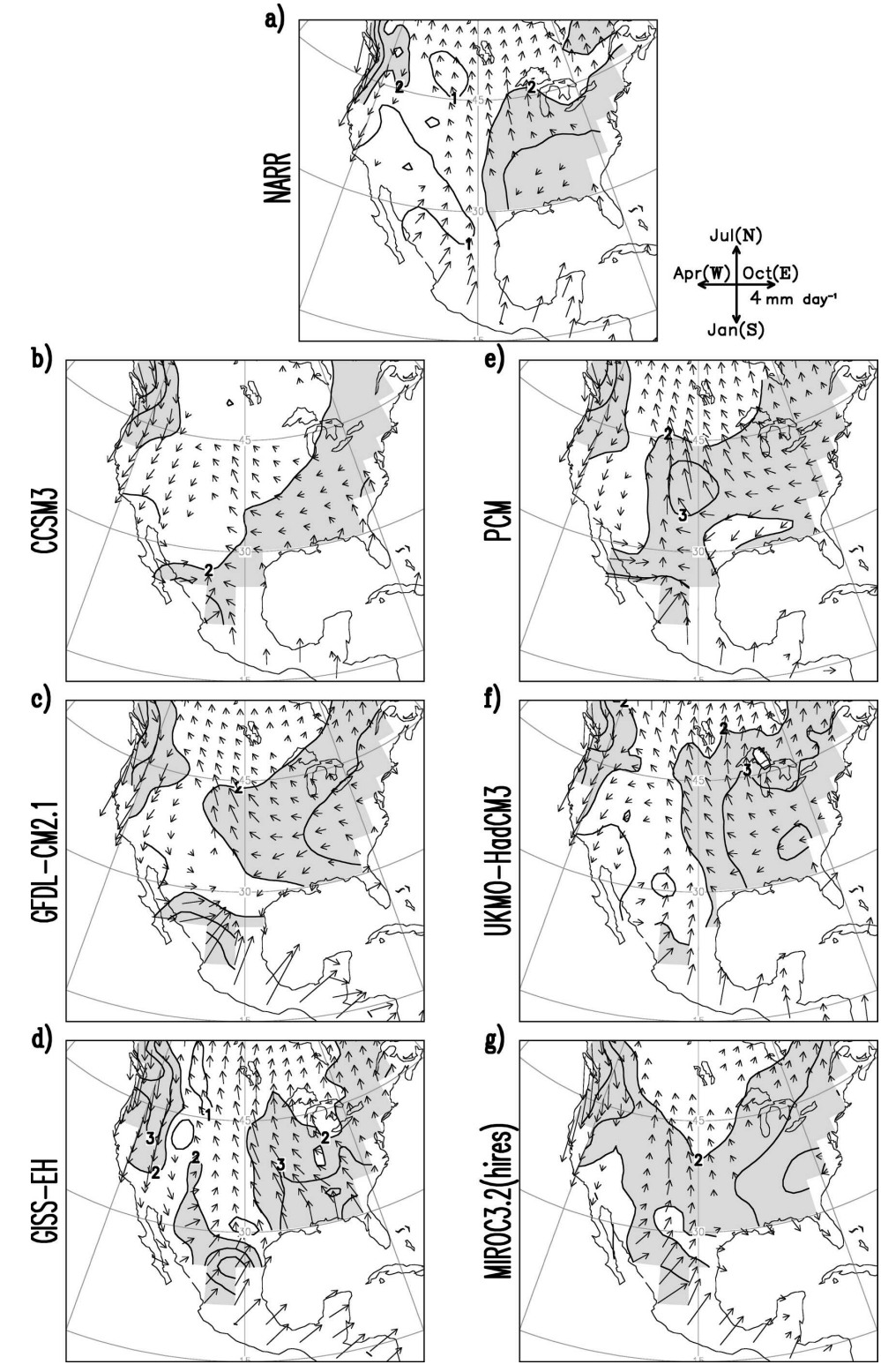
a)
NARR
Jul(N)
Apr(W) Oct(E)
4 mm day⁻¹
Jan(S)
b)
CCSM3
e)
PCM
c)
GFDL-CM2.1
f)
UKMO-HadCM3
d)
GISS-EH
g)
MIROC3.2(hires)

Models display differing degree of accuracy when portraying the annual cycle of precipitation (Figs. 1b–g). While all the models capture the timing of the winter maximum over the northwestern United States, they exhibit some difficulty in capturing the timing of the summer maxima over the central United States and Mexico. The annual cycle from tropical Mexico to the central United States peaks erroneously from late spring to early summer in both CCSM3 and PCM; the amplitudes are more realistic in the former than in the latter. The rest of the models have a better timing in that region, specially MIROC3.2(hires). The observed weak maximum in late winter–early spring over the southern United States and the weak annual cycle over the eastern U.S. coast pose additional problems for the models as well. Those features are captured a bit later and are too strong in the spring, in particular for GISS-EH which peaks even later in the summer.

The structure of the mean annual precipitation by the models has similar results than those in the annual cycle. Simulations are reasonable over the northwestern United States, with a winter maximum, but are problematic to the east of the Continental Divide, which has winter (over the southern United States) and summer (over the central United States and Mexico) maxima. The UKMO-HadCM3 model has the best reproduction of the observed features. Figures not displayed for winter and summer means show the difficulty the rest of the models have in reproducing the winter maximum of precipitation over the southern United States as well as the distribution of precipitation over the central United States during the summer.

4. Precipitation variability

A first look at precipitation variability is made through a glimpse of the mean standard deviation of precipitation during the warm-season months (JJA; Fig. 2). Emphasis is made on the continental features of the field, although considerable differences exist over the oceans. North America is characterized by two regions of maximum precipitation variability ($\geq$1.5 mm day^{-1}): one over the central United States and the other over eastern Mexico (Fig. 2a).

Models have limited success locating these maxima of precipitation variability (Figs. 2b–g). The maximum over the central United States is present but shifted to the southwest in all the simulations, while the maximum over eastern Mexico is almost absent, with the exception of the UKMO-HadCM3 and GISS-EH simulations. Precipitation variability over the United States reaches a maximum in the GFDL-CM2.1 simulation, and a minimum in the PCM simulation.[5]

Knowing the relative success of the models in simulating the maximum of variability over the central United States, the study now will focus on this region.

a. Great Plains Precipitation index

The area exhibiting the local maximum in observed precipitation variability over the central United States (Fig. 2a) defines a coherent domain that can be used to study the temporal variability of the region (Ruiz-Barradas and Nigam 2005, 2006). The 10° latitude–longitude box (35°–45°N, 100°–90°W) encompasses the region. The areal average of precipitation anomalies in the box defines the Great Plains Precipitation (GPP) index for the warm-season months (JJA).

The GPP index in simulations is also defined in terms of area-averaged precipitation anomalies over the 10° latitude–longitude region defined from observations. Although the box does not entirely enclose the local maximum of standard deviation in the individual simulations, it is not much of a problem for the analysis. The alternate 10° box draw in the GFDL-CM2.1 panel (dashed box in Fig. 2c) is used for a sensitivity analysis to test the dependence of the results on the choice of

[5] Large variability over the northwestern coast of Mexico and southwestern United States seems to be a problem for PCM and GFDL-CM2.1 models and probably, as suggested by the massive incursion of precipitation from the Pacific Ocean over the continent, due to a very active intertropical convergence zone in the eastern Pacific.

←

FIG. 1. First harmonic of climatological precipitation and mean annual precipitation in reanalysis and coupled simulations (1979–98): (a) NARR, (b) CCSM3, (c) GFDL-CM2.1, (d) GISS-EH, (e) PCM, (f) UKMO-HadCM3, and (g) MIROC3.2(hires). Vectors represent the first harmonic while background isolines display the mean annual precipitation in mm day^{-1}. The insert vectors at the top of the figure indicate the scaling of the magnitude in mm day^{-1} and the phase of the annual cycle: vectors pointing to the south indicate a maximum on 1 January, pointing to the west means a maximum on 1 April, pointing toward the north indicates a maximum on 1 July, and pointing to the east means a maximum on 1 October. Only magnitudes of the annual cycle equal to or larger than 0.5 mm day^{-1} are displayed. Mean annual precipitation is contoured at the 1, 2, 3, 4, 6, and 9 mm day^{-1} isolines. Shading indicates mean annual precipitation equal or larger than 2 mm day^{-1}.

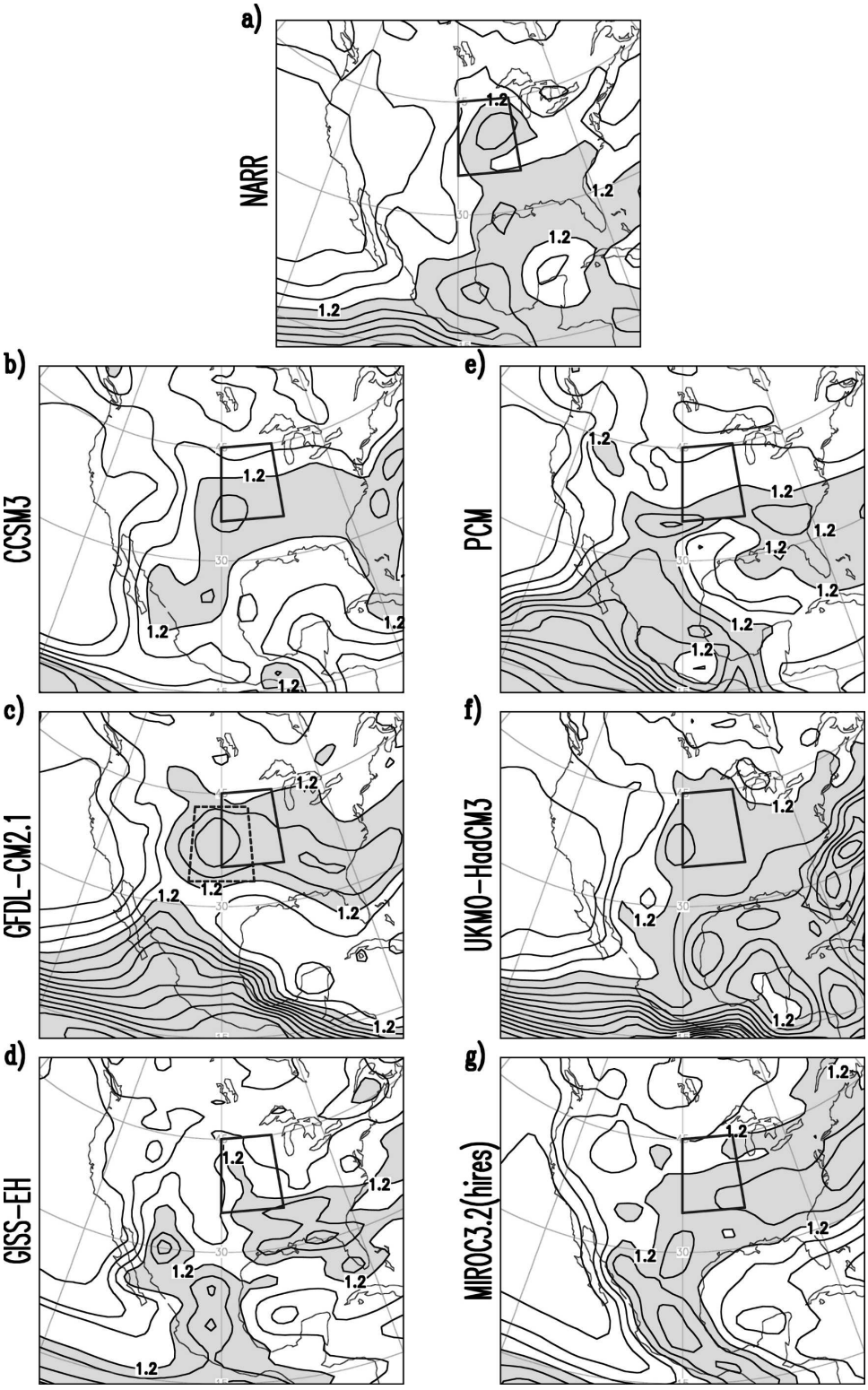

FIG. 2. Standard deviation of monthly precipitation anomalies during summer (JJA) in reanalysis (1979–98) and coupled simulations (1951–98): (a) NARR, (b) CCSM3, (c) GFDL-CM2.1, (d) GISS-EH, (e) PCM, (f) UKMO-HadCM3, and (g) MIROC3.2(hires). The marked box with continuous lines delineates the Great Plains region defined by the maximum in observed precipitation variability in (a). The box made of dashed lines in (c) contours the region of maximum precipitation variability for the GFDL model that is used for a sensitivity analysis. The contour interval is 0.3 mm day^{-1} and values equal to or greater than 1.2 mm day^{-1} are shaded.

TABLE 1. Monthly JJA SD of the GPP index in the 1951–98 period.

	U.S.–Mexico dataset	CCSM3	GFDL-CM2.1	GISS-EH	PCM	UKMO-HadCM3	MIROC3.2 (hires)
JJA SD	0.91	1.00	1.12	0.72	0.63	0.92	0.78

the region defining the GPP index (refer to the appendix for the analysis).

Realistic monthly precipitation variability over the Great Plains is difficult for models to capture. Correlation between observed and simulated monthly GPP indices is almost nonexistent (−0.13 the highest). A compact, and more favorable measure of the variability is given by the mean standard deviation (SD) of the monthly GPP index. In this comparison the U.S.–Mexico dataset is preferred to the NARR dataset because of the shorter period of the latter.[6] With an observed variability over the Great Plains region of 0.91 mm day^{-1}, Table 1 summarizes variability over the region: large variability in the GFDL-CM2.1 simulation (SD = 1.12 mm day^{-1}), low variability in the PCM simulation (SD = 0.63 mm day^{-1}), and nature-matching variability in the UKMO-HadCM3 simulation (SD = 0.92 mm day^{-1}); the CCSM3 simulation is the second closest to the observed variability (SD = 1.00 mm day^{-1}).

The proximity of simulated SD to the observed one is not a guarantee of an exact match of observed distribution of wet and dry months. Frequency of months with precipitation above (wet) or below (dry) climatology is calculated from monthly GPP indices and is displayed as a histogram in bins of 0.5 mm day^{-1} (Fig. 3). The observed U.S.–Mexico dataset indicates a higher number of dry months (76) than wet months (68), largely confined to the ±1.5 mm day^{-1} range. The number of dry and wet months partially holds for the simulations, except for PCM, which has more wet (77) than dry (67) months, and UKMO-HadCM3, which has an equal number of wet and dry (72) months. It is apparent that the smaller the warm-season SD, the larger the number of months concentrated in the ±0.5 mm day^{-1} range [e.g., PCM, GISS-EH, and MIROC3.2(hires)]. Large warm-season SD, as in the GFDL-CM2.1 simulation, implies the presence of months with large negative (≥|−3| mm day^{-1}) and positive (≥4 mm day^{-1}) precipitation anomalies. Alternatively, UKMO-HadCM3, and CCSM3 perform better than the other models in the ±1 mm day^{-1} range, but do not show the observed marked decline in wet months from the 0.5–1 to the 1.5–2 mm day^{-1} range.

b. Season-mean GPP index

It is expected that season-mean indices will demonstrate better correspondence with observations than the monthly indices. Attention is now shifted to smoothed versions of the monthly indices (Fig. 4). The smoothing is done via a 1–2–1 filter of the summer-mean index anomalies; in this way, the preceding, current, and subsequent summer means are included in the calculation of the smoothed index enhancing interannual variability in them. Plotted indices come from the U.S.–Mexico dataset (continuous black line), the NARR dataset (dashed black line), and simulations (color lines).

Temporal variability of the smoothed GPP index from observations is not easily reproduced by simulations. The proximity between indices from the U.S.–Mexico and the NARR datasets is evidence of the successful assimilation of precipitation in NARR.[7] Both indexes capture the 1993 flood event and 1998 dry event over the central United States; other dry episodes are also evident during the mid 1950s and first half of the 1970s in the index from the U.S.–Mexico dataset. The only model capturing the 1993 wet event, as well as the 1988 and early 1970s dry events is the UKMO-HadCM3 (purple line); however, the 1993 event in the model starts earlier than observed.

Temporal correlations between the observed and simulated smoothed indices are displayed in Table 2. It summarizes the synchronous temporal evolution of the GPP indices contained in Fig. 4: simulations by GFDL-CM2.1 (dark green line), CCSM3 (red line), and MIROC3.2(hires) (yellow–green line) have very limited correlation with observations; PCM (orange line), and GISS-EH (blue line) have modest correlation, and UKMO-HadCM3 (purple line) has a reasonable high correlation of 0.54. While it is not possible to attest to the statistical significance of the correlations of the majority of the models, correlations with observations us-

[6] Correlation between NARR and U.S.–Mexico GPP indices is 0.99 for the common 1979–98 period.

[7] Differences between GPP indices from U.S.–Mexico and NARR datasets are minimum, or nonexistent, if the index from the U.S.–Mexico dataset is calculated with respect to the 1979–98 climatology.

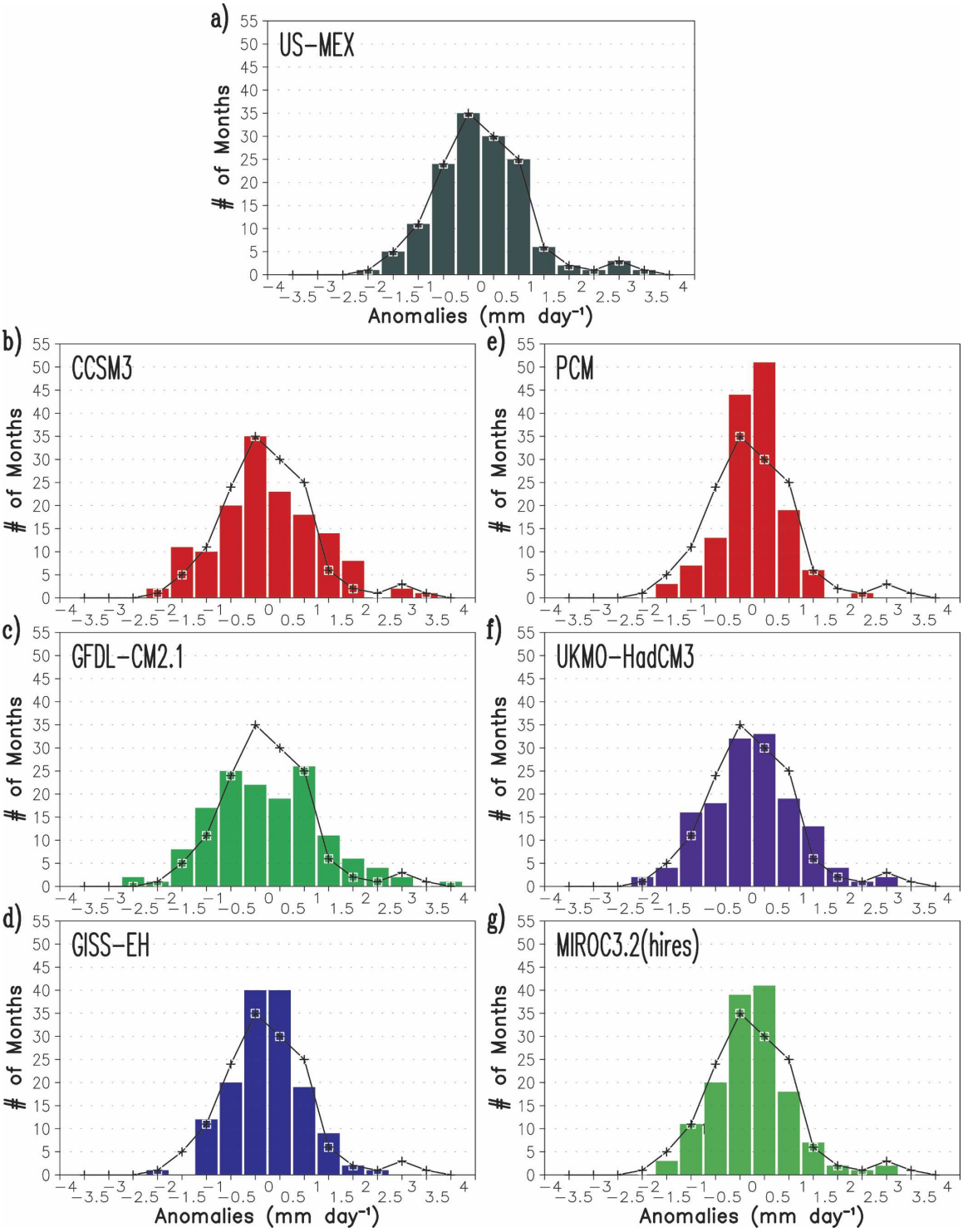

FIG. 3. Histogram of precipitation events over the Great Plains as portrayed by the GPP index from (a) the U.S.–Mexico dataset, (b) CCSM3, (c) GFDL-CM2.1, (d) GISS-EH, (e) PCM, (f) UKMO-HadCM3, and (g) MIROC3.2(hires). For comparison purposes, the histogram from the U.S.–Mexico index has been plotted as a black line in all panels. The *x* axis represents the anomalous events by categories of 0.5 mm day^{-1} and the *y* axis shows the number of months that a given category of anomalies occurs.

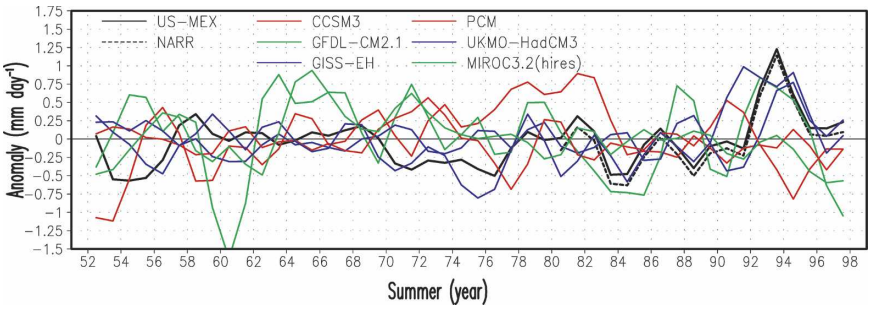

FIG. 4. Smoothed GPP index anomalies during the warm season (JJA) in observations and coupled simulations: U.S.–Mexico (observed rain gauge), continuous black line; NARR, dashed black line; CCSM3, red line; GFDL-CM2.1, dark green line; GISS-EH, blue line; PCM, orange line; UKMO-HadCM3, purple line; MIROC3.2(hires), yellow–green line. The smoothed index is obtained from a 1–2–1 averaging of the summer-mean anomalies. The monthly, warm-season SD, and correlations among the smoothed precipitation indices are displayed in Tables 1 and 2, respectively.

ing GISS-EH (0.34) and UKMO-HadCM3 (0.54) models are statistically significant with 95% confidence.

5. Structure and linkages of precipitation variability

In this section the structure and linkages of precipitation variability with the atmospheric water balance components over the Great Plains in the models are contrasted with observations (via the regional reanalysis) as in Ruiz-Barradas and Nigam (2005). At stake is the comparative significance of those components (and processes) in models and observations. The monthly GPP index is regressed against monthly precipitation, stationary horizontal moisture fluxes (from winds and specific humidity), and evapotranspiration (from surface latent heat) for the warm-season months (JJA) during the 1979–98 period for NARR, and for the 1951–98 period for simulations. A statistical significance at the 0.05 level is implied by the shading in the figures.

a. Precipitation

The GPP index regressions against precipitation anomalies from the regional reanalysis and simulations are displayed in Fig. 5 with a contour interval of 0.3 mm day^{-1}. Due to the definition of the GPP index, it is not surprising that the structure of precipitation anomalies in the regional reanalysis is confined to the Great Plains region without detriment to precipitation over other continental regions[8] (Fig. 5a).

Regressed simulated precipitation anomalies show a consistent and confined structure in precipitation anomalies with a maximum over the focus region of the Great Plains (Figs. 5b–g). The exception to this is the CCSM3 simulation whose precipitation structure extends meridionally too far to the south into Mexico; the meridional elongation is also present in the PCM simulation, although to a much lesser extent. It is also interesting to note that, except for the UKMO-HadCM3, all the models imply a decrease of precipitation over northwestern Mexico.

b. Moisture fluxes

Vertically integrated stationary moisture flux anomalies[9] and their convergences associated with the regressed precipitation anomalies from the regional reanalysis and simulations are shown in Fig. 6; as in precipitation regressions, the contour interval of 0.3 mm day^{-1} is used for moisture flux convergence. Great Plains precipitation variability in the regional reanalysis

[8] The significance of precipitation anomalies over oceanic regions is beyond the scope of the present study.

[9] Stationary fluxes refer to moisture transports by the monthly mean circulation.

TABLE 2. Correlations among smoothed GPP indices in the 1951–98 period. The values set in bold indicate a significance of the correlation at the 0.05 level following a Student's *t* test.

	U.S.–Mexico dataset	CCSM3	GFDL-CM2.1	GISS-EH	PCM	UKMO-HadCM3	MIROC3. 2 (hires)
U.S.–Mexico dataset	1	−0.11	0.10	**0.34**	−0.25	**0.54**	−0.11

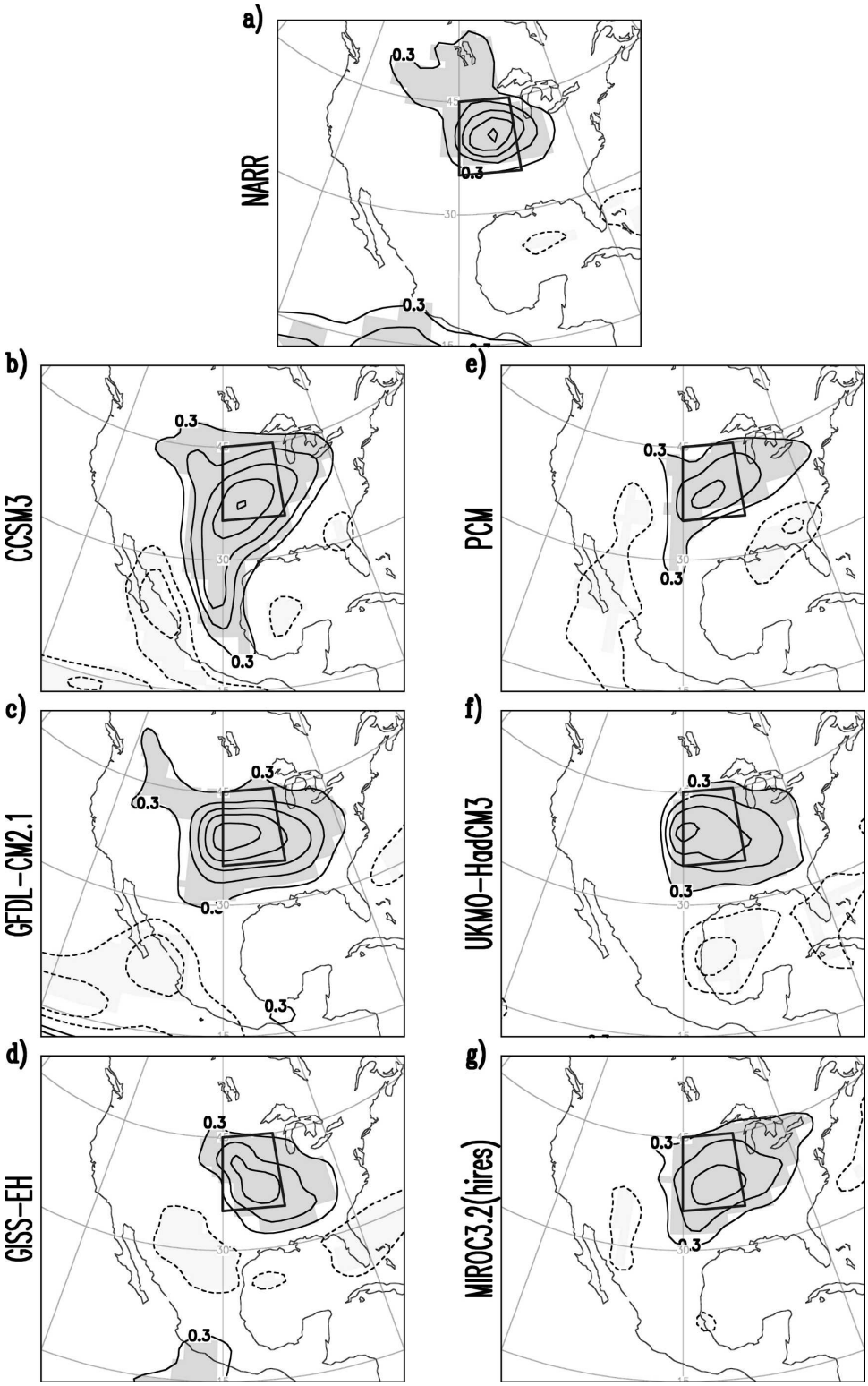

FIG. 5. Warm-season regressions of the GPP index on precipitation anomalies from (a) NARR, (b) CCSM3, (c) GFDL-CM2.1, (d) GISS-EH, (e) PCM, (f) UKMO-HadCM3, and (g) MIROC3.2(hires). The index and regressions are from the same monthly JJA dataset, in each case. Contour interval is 0.3 mm day^{-1}. Dark (light) shading denotes areas of positive (negative) rainfall anomalies statistically significant at the 0.05 level; the zero contour is omitted.

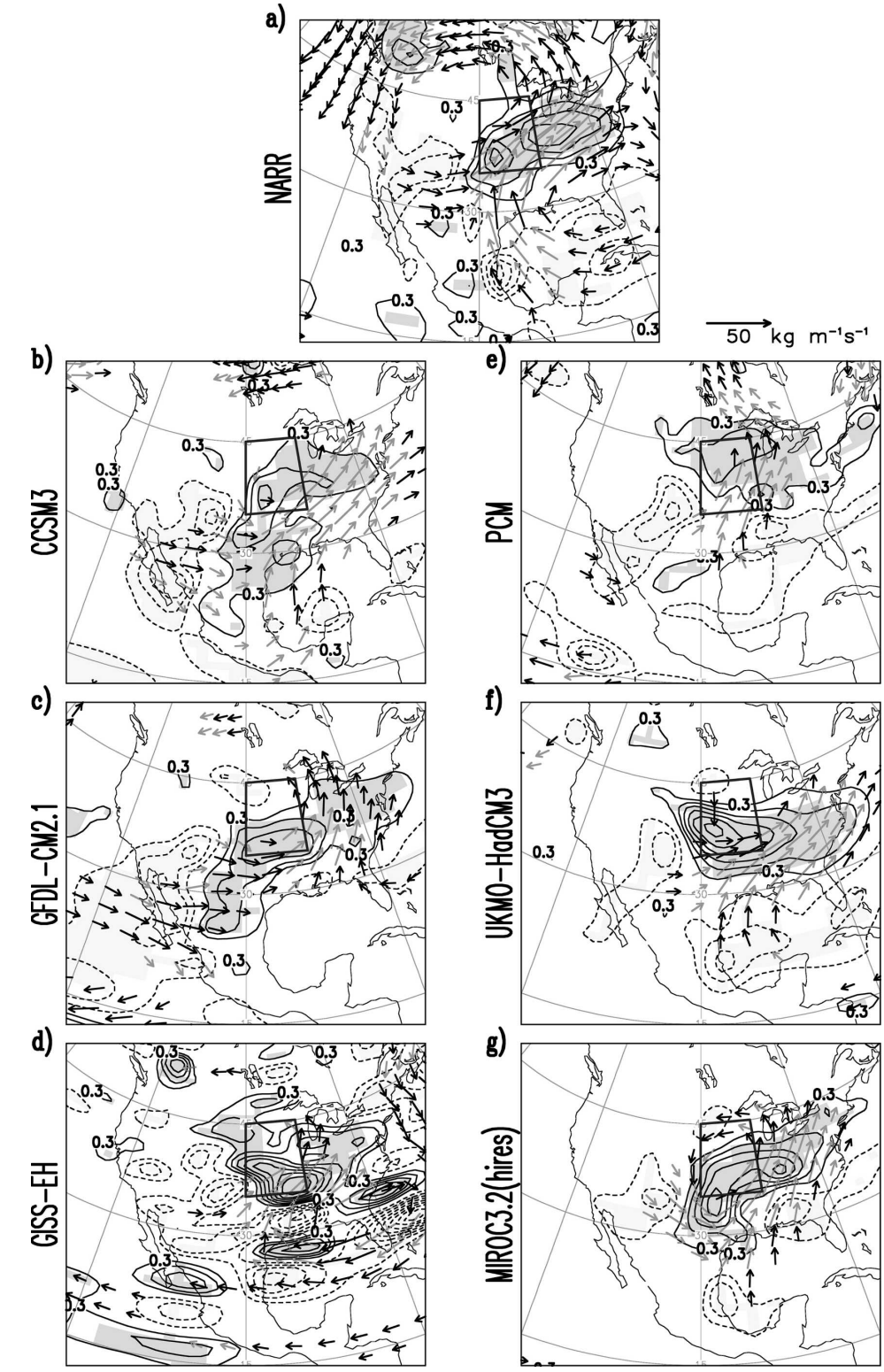

FIG. 6. Same as in Fig. 5, but on stationary moisture flux anomalies. Moisture flux convergence is displayed as contours. Moisture fluxes and corresponding flux convergence anomalies are vertically integrated (300 hPa–surface). Shading and contour interval are as in Fig. 5. Positive–negative anomalies represent moisture flux convergence–divergence anomalies. Fluxes smaller than 10 kg m^{-1} s^{-1} have been masked out and those statistically significant at the 0.05 level have been drawn with a lighter color.

is largely supported by the convergence of stationary moisture fluxes; this apparently accounts for up to three-fourths of the precipitation over the Great Plains (Fig. 6a). A coherent, anomalous anticyclonic circulation carries moisture northward from the Gulf of Mexico and the Caribbean Sea. An anomalous cyclonic circulation over the western half of the United States prompts a weaker connection to the Pacific, via westerly fluxes over the southwestern states.

Regressed simulated moisture flux anomalies, and their convergences, have less in common (Figs. 6b–g) than the precipitation anomalies but still manage to have a maximum of moisture flux convergence over the focus region. Moisture fluxes from the Gulf of Mexico into the central United States are apparent in GISS-EH, PCM, UKMO-HadCM3, and MIROC3.2(hires) simulations; the Caribbean connection, although weak, is present only in the UKMO-HadCM3 simulation. The connection to the Pacific via westerly fluxes over the southwestern states in NARR is also weak in simulations; none of the models simulate the anomalous cyclonic circulation over the United States, with the exception of MIROC3.2(hires) but not with the extension present in the regional reanalysis. However, CCSM3 and, in particular, GFDL-CM2.1 simulations put a premium on moisture fluxes from the Pacific into the central United States; while GFDL-CM2.1 has very weak moisture fluxes from the Gulf of Mexico (smaller than 10 kg m^{-1} s^{-1}, see caption for details), CCSM3 also has them but they are driven by activity in the Pacific.

The structure of the simulated moisture flux convergence in the models is less consistent among the different simulations than it was in the simulated precipitation. Distributions of moisture flux convergence over the Great Plains range from the noisy and very large in GISS-EH, to the almost identical to the regional reanalysis by MIROC3.2(hires); simulated moisture flux convergence by UKMO-HadCM3 is also larger than that in NARR, while those by CCSM3, GFDL-CM2.1, and PCM are slightly weaker than in the regional reanalysis. Note that the simulated moisture flux divergence over northwestern Mexico seems to explain the simulated (and not observed) reduced precipitation over that region, especially in CCSM3, GFDL-CM2.1, and PCM.

c. Evaporation

The GPP index regressions on surface evaporation anomalies from the regional reanalysis and simulations are displayed in Fig. 7; here we are using the word "evaporation" to refer to the sum of evaporation from wet bare soil and canopy plus transpiration from vegetated surfaces. In this case, the 0.1 mm day^{-1} contour interval is a third of that used for precipitation and moisture flux convergence. Evaporation anomalies in the regional reanalysis are modest over the Great Plains region (Fig. 7a) and noticeably smaller than precipitation and moisture flux convergence anomalies.

Regressed simulated evaporation anomalies also have few similarities among them (Figs. 7b–g). Great Plains evaporation anomalies span from zero, or close to zero, in GISS-EH to very large anomalies in CCSM3 and GFDL-CM2.1; evaporation anomalies in PCM, UKMO-HadCM3, and MIROC3.2(hires) are modest. The maximum in evaporation anomalies in regional reanalysis and simulations is shifted toward the southwest, with respect to the maximum in precipitation anomalies. Note the closeness of the structures between precipitation and evaporation anomalies simulated by CCSM3 and GFDL-CM2.1.

d. Relative contributions

The previous description of regressed anomalies of the main water balance components in the atmosphere indicates a different hierarchy of processes that are important for precipitation variability over the Great Plains in observations (NARR) and the different models. Although it is important to have a well-simulated structure of anomalies, it is even more important to have the relative contributions of the processes responsible for precipitation variability as identified in observations. Observations, via the regional reanalysis, indicate that precipitation anomalies over this region are mostly due to convergence of remote moisture fluxes, and to a smaller extent due to local evaporation of previous precipitation. Thus, attending to the magnitude of the maximum anomalies, models seem to emphasize different processes as follows. In the first type of models (e.g., CCSM3 and GFDL-CM2.1), the emphasis is on the large local recycling of precipitation. In the second type of models (e.g., GISS-EH), the emphasis is on the remote sources of water inducing large moisture flux convergence. In the third type of model [e.g., UKMO-HadCM3, MIROC3.2(hires), and PCM], the emphasis is still on the remote sources of water converging over the region but the local recycling of precipitation increases its role, similar to observations.

Another way to see these contributions is by taking an area average of the regressed anomalies of precipitation, vertically integrated moisture flux convergence, and evaporation over the Great Plains region (35°–45°N, 100°–90°W) as seen in Table 3. In the regional reanalysis, moisture flux convergence dominates over modest evaporation in the generation of precipitation; the former accounts for up to three-fourths of precipitation, while the latter accounts for up to a quarter of

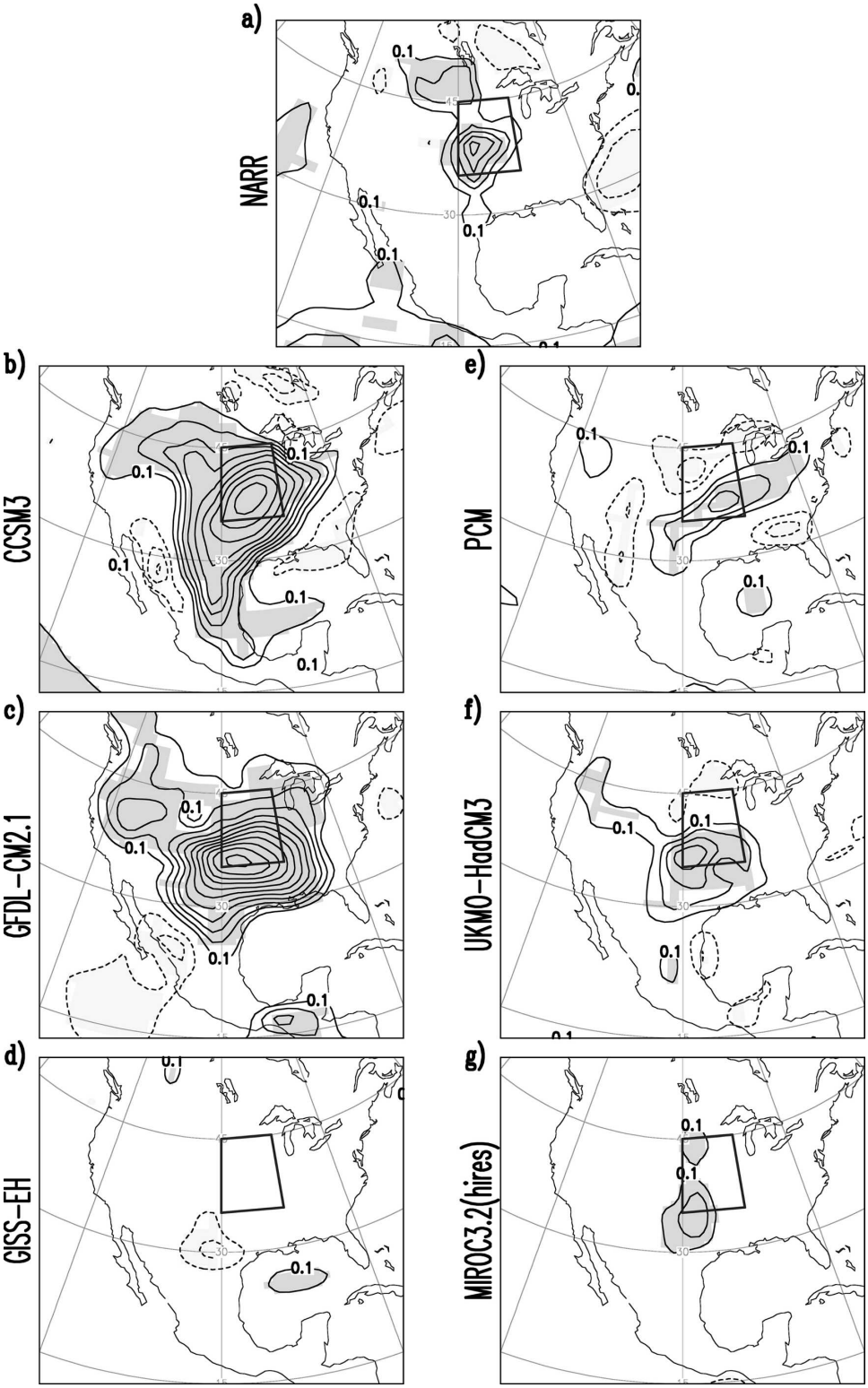

FIG. 7. Same as in Fig. 5, but on evaporation anomalies. Contour interval is 0.1 mm day^{-1}; dark (light) shading denotes areas of positive (negative) evaporation anomalies statistically significant at the 0.05 level; the zero contour is omitted.

TABLE 3. Area-averaged regressed anomalies of precipitation (P), vertically integrated moisture flux convergence (MFC), and evaporation (E) over the Great Plains (35°–45°N, 100°–90°W) in mm day^{-1}.

	P	MFC	E
NARR	0.89	0.66	0.22
CCSM3	1.04	0.45	0.69
GFDL-CM2.1	1.13	0.40	0.59
GISS-EH	0.73	0.91	−0.04
PCM	0.63	0.46	0.04
UKMO-HadCM3	0.92	0.83	0.14
MIROC3.2(hires)	0.78	0.66	0.06

the precipitation. Area averages of the regressed simulated anomalies also highlights the three different kind of models.[10] However, models are distributed in a slightly different manner than before. Models where large evaporation dominates over moisture flux convergence in the generation of precipitation are CCSM3 and GFDL-CM2.1. Models where moisture flux convergence dominates over reduced evaporation are GISS-EH, PCM, and MIROC3.2(hires). The only model where moisture flux convergence dominates over modes evaporation in the generation of precipitation, as in the regional reanalysis, is UKMO-HadCM3.

6. Precipitation recycling

The local recycling of precipitation via land surface processes depends on antecedent precipitation and the characteristics of the land surface over the region. It is apparent from the previous sections that the models have different degrees of recycling, but it is not clear how much memory they carry from past precipitation. While the recycling of precipitation may be high, it can be a slow or rapid process depending on the land surface processes that put back the precipitated water into the atmosphere. Slow recycling of precipitation has a stronger link with antecedent precipitation than fast recycling does, or in other words, carries more memory from past precipitation. An estimation of this memory can be established by an autocorrelation analysis of precipitation. The analysis is carried out on the monthly GPP indices calculating the correlation between July's precipitation anomalies and the May, June, July, and August precipitation anomalies for the 1951–98 period

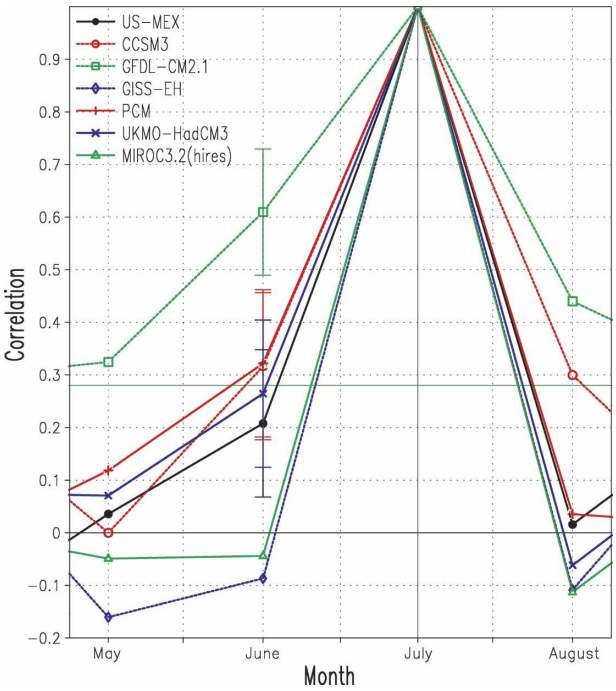

FIG. 8. Correlation between July's GPP anomalies with May, June, July, and August monthly precipitation anomalies for the 1951–98 period. Correlations from the retrospective U.S.–Mexico precipitation analysis are shown using filled black circles; CCSM3, open red circles; GFDL-CM2.1, open green squares; GISS-EH, open blue diamonds; PCM, orange plus signs; UKMO-HadCM3, purple multiplication signs; MIROC3.2(hires), open yellow–green triangles. The horizontal light blue line marks the critical correlation at the 0.05 significance level according to the Student's t test. Error bars in the June correlation for the U.S.–Mexico dataset and models represent the *standard error* when calculating the correlation.

(Fig. 8). July's precipitation dependence on previous months' precipitation in observations from the U.S.–Mexico dataset (black line) indicates a low correlation (~0.2 with June and lower with earlier months); August's precipitation dependence on July's precipitation is almost nonexistent (~0.02). The observed low dependence on previous months' precipitation defines a narrow spikelike graph suggesting weak memory of past precipitation over the Great Plains. Thus, a broader/narrower JJA spike than the one from observed data will indicate even higher/lower correlations as well as stronger/weaker memory of antecedent precipitation.

The dependence of precipitation on that of the previous month in simulations adds another element to the discussion of the previous section. The autocorrelation of the GPP indices simulated by GFDL-CM2.1 (dashed dark green line) and CCSM3 (dashed red line) have a broader spike than that of the observed index (correlations are at least 0.3 on both sides of the maximum in

[10] Note that taking the area average of the anomalies with different signs in the region can generate the wrong impression, as it is the case for moisture flux convergence from GFDL-CM2.1, evaporation from UKMO-HadCM3, and especially, from PCM (which has comparable negative and positive anomalies).

July); however, correlations with the GFDL-CM2.1 index are notoriously higher than those with the CCSM3 index (in spite of the larger mean evaporation anomalies in CCSM3). The autocorrelation of the GPP indices simulated by GISS-EH (dashed blue line) and MIROC3.2(hires) (yellow–green line) have narrower spikes than that from the observed index (correlations are around −0.1 on both sides of the maximum in July). Finally, the autocorrelation of the GPP indices simulated by UKMO-HadCM3 (purple line) and PCM (orange line) have comparable spikes to the spike from the observed index, even though PCM has low mean evaporation.

A Student's *t* test at the 0.05 level reveals that only correlations larger than $|\pm 0.28|$ are statistically significant; thus, autocorrelations from GFDL-CM2.1, CCSM3, and PCM indices are the only ones that satisfy this statistical constrain. However, because there is a *standard error* associated with the correlations, it is not possible to rule out the statistical significance of the June–July correlations in UKMO-HadCM3 and U.S.–Mexico indices when considering that their standard error makes their correlations surpass the critical correlation.

The idea behind a high correlation at a 1-month lag of a precipitation index is that precipitation in the previous month is stored in the upper layers of the soil and then transpired from the vegetated surface to provide the needed moisture for precipitation in the current month; it is there that the memory of antecedent precipitation resides. Thus, one could expect to have large evaporation anomalies, from canopy transpiration, associated with large correlations at a 1-month lag of the precipitation index, as it is the case for the GFDL-CM2.1 model. However, when significant precipitation is not reaching the ground but it is intercepted by the canopy, precipitation can be quickly evaporated from the wet canopy and the memory of the soil is lost to some extent; in this case, the dependence of the current month's precipitation on the previous months precipitation is reduced. Thus, large evaporation anomalies, from a wet canopy, cannot be expected to be associated with large correlation at a 1-month lag of the precipitation index, as it is the case for the CCSM3 model (see also Wu and Dickinson 2005).

In those models where evaporation anomalies are small there is not much memory from the moisture of the soil to be passed from 1 month to another via transpiration of the canopy, so the 1-month lag correlation of their precipitation index is very low, as it is the case for GISS-EH and MIROC3.2(hires).

Interestingly, some of the models (or their earlier versions) analyzed here have been key to recent claims of strong coupling between soil moisture and precipitation, or "hot spots" (Koster et al. 2004). The claims are based on the Global Land–Atmosphere Coupling Experiment (GLACE; see online at http://glace.gsfc.nasa.gov) where the coupling strength in twelve atmosphere–land surface models was analyzed. Surprisingly, the GLACE conclusion regarding hot spots is drawn by averaging the sensitivities of 12 models. The 12-model average is, of course, easily impacted by the large signals of a few models that makes the multimodel average unrepresentative of the analyzed model population. There is evidently considerable scatter in the strength of land–atmosphere coupling in the GLACE models, especially over the central United States (cf. Fig. 1 in Koster et al. 2004). While the GFDL model has one of the strongest couplings, the atmospheric components of CCSM3 and UKMO-HadCM3 present a much weaker coupling (Fig. 5 in Koster et al. 2006), in line with the results presented here.

7. Concluding remarks

The present study has sought to ascertain the structure of warm-season hydroclimate variability over the U.S. Great Plains and the extent to which the observed variability features are represented in the state-of-the-art climate simulations of the twentieth century. The focus is on the analysis of interannual variability where models are more challenged, however, attention is briefly focused on the simulated annual cycle of precipitation too.

The analysis is largely based on, and driven by, previous research from the authors warm-season hydroclimate variability studies over North America in AMIP simulations and observations at seasonal and interannual time scales. Curiosity arises not only because the difficulties that some of the state-of-the art atmospheric GCMs show in capturing the annual cycle of precipitation (Nigam and Ruiz-Barradas 2006), but also in the difficulties that those models have capturing the relative contributions by anomalous moisture fluxes and evaporation important to the generation of precipitation variability over the Great Plains (Ruiz-Barradas and Nigam 2005, 2006).

There is a big interest in identifying those problems in fully coupled GCMs over the season and region because the potential use of their simulations for future climate change scenarios. In the current study four American models from NCAR (CCSM3 and PCM), NOAA (GFDL-CM2.1), and NASA (GISS-EH), a British model (UKMO-HadcCM3), and a Japanese model [MIROC3.2(hires)] are analyzed in the context of Great Plains hydroclimate variability during the

warm-season (JJA). Comparisons are made against NCEP's North American Regional Reanalysis, and the U.S.–Mexico analyzed precipitation dataset.

The annual cycle of precipitation, and mean annual precipitation present a surprising challenge to the models (considering that model tuning is usually made with the observed annual cycle).

- Climatological winter precipitation is reasonably well simulated over the U.S. northwest. Models simulate reasonably well the annual cycle over the northwestern United States and its mean annual precipitation while they fail to capture the weak annual cycle over the southeastern United States and its mean annual precipitation; precipitation in those regions peaks during middle and late winter, respectively.
- Climatological summer precipitation is more demanding. Models have problems capturing both mean precipitation and its annual cycle over the central United States and Mexico, which peaks in summer. Models like CCSM3, GFDL-CM2.1, and PCM have the annual cycle in the central United States and Mexico markedly ahead of time. In general, UKMO-HadCM3 is closer to observations than the others but it is not perfect, especially in regards of the features over the southeastern United States where the annual cycle is a bit stronger than observations indicate.

Interannual variability of precipitation and its links to the atmospheric water balance components are centered around the Great Plains Precipitation (GPP) index. The index is objectively constructed on the basis of the standard deviation distribution of observed monthly precipitation in the warm-season months. This maximum in standard deviation of precipitation in general is displaced southwestward in the simulations with respect to the observed maximum. While the region defining the Great Plains (35°–45°N, 100°–90°W), and the GPP index, is based on the position of the maximum of standard deviation in observations, it is shown (in the appendix) that using the region defined by the maximum in standard deviation of simulated precipitation only strengthens the validity of the results summarized in the following paragraphs.

- Model evolution is problematic. Simulated monthly GPP indices are temporally uncorrelated with the observed monthly GPP index. Smoothing of the indices, to enhance interannual variability, only marginally increases the correlation between observed and simulated smoothed indices, except for the UKMO-HadCM3 model that has a statistically significant correlation of 0.54.
- Large precipitation variability is consequence of the occurrence of rare extreme wet and/or dry events (as in GFDL-CM2.1), while reduced precipitation variability is the consequence of the lack of those extreme events and the increased number of small wet and/or dry events (as in PCM).

The relative importance of processes contributing to the generation of interannual variability of precipitation over the Great Plains in the warm season is compared in observations and simulations. Autocorrelation analysis of the monthly GPP indices and their regressed water balance components indicate the following hierarchy of processes in the models:[11]

- In models like UKMO-HadCM3 and PCM, moisture flux converging from the Gulf of Mexico into the region is more important than local evapotranspiration of preceding precipitation, as in the NARR results. Precipitation variability as well as the structure of anomalies of the water balance components in the UKMO-HadCM3 model are closer to observations than those in the rest of the models.
- In models like GISS-EH and MIROC3.1(hires) the gap between contributions by moisture flux convergence and local evapotranspiration is increased by means of increasing moisture flux convergence from the Gulf of Mexico, and diminishing (reducing to near zero in GISS-EH) the local recycling of preceding precipitation via evaporation.
- In the GFDL-CM2.1 model the local recycling of preceding precipitation via evapotranspiration is larger than the convergence of moisture fluxes from remote regions. This model emphasizes more moisture fluxes from the Pacific than from the Gulf of Mexico—not a feature present in the NARR results. The CCSM3 model behaves similarly to GFDL-CM2.1 model, however, its land surface memory is weaker.

This study emphasizes the importance of remote water sources (moisture fluxes) over local land surface processes (evapotranspiration) in the generation of Great Plains precipitation variability during the warm-season months. This is clearly evident in observations represented by the regional reanalysis but only in some global models. Our finding on excessive land–atmosphere interactions in some models are consistent with GLACE results pertaining to these models, but not

[11] Evaluations of GFDL-CM2.0, GISS-AOM, and GISS-ER models indicate that in the first two models the local recycling of precipitation is the main process of precipitation variability, while in the third model convergence of moisture fluxes is the most important and overwhelming process for generating precipitation variability over the Great Plains in the warm-season months.

supportive of the drawn conclusion on the existence of a strong coupling over the central United States. Regardless of the statistical significance in the present analysis, the physical insight is very consistent. An enhanced (neglected) recycling of precipitation implies substantial (reduced) energy going into the regional land surface component of the models. Investigation of this issue is already under way as well as analysis of precipitation variability during the cold-season months, where evaporation plays less of a role and models seem to be doing better (at least over the U.S. northwest). This will improve the understanding of the water and energy cycles over the region.

The Hadley Centre's model is the one that better approaches NARR's hydroclimate variability over the Great Plains during the warm season. This model will be used to assess the impact of global climate change scenarios over the region in an upcoming analysis.

Acknowledgments. This research was funded by NSF and DOE as a Climate Model Evaluation Project (CMEP) Grant NSF ATM-0445136, under the U.S. CLIVAR Program (http://www.usclivar.org/index.html). We also want to thank the international modeling groups for providing their data for analysis, the Program for Climate Model Diagnosis and Intercomparison (PCMDI) for collecting and archiving the model data, the JSC/CLIVAR Working Group on Coupled Modelling (WGCM) and their Coupled Model Intercomparison Project (CMIP), the Climate Simulation Panel for organizing the model data analysis activity, and the IPCC WG1 TSU for technical support. The IPCC Data Archive at Lawrence Livermore National Laboratory is supported by the Office of Science, U.S. Department of Energy. We want to express our gratitude to Andy Pitman (Editor) for his encouraging words and comments on the manuscript. We would also like to thank Adam Schlosser, and an anonymous reviewer, for their constructive comments that helped to improve the quality of the manuscript. We also would like to thank Renu Joseph for archiving and homogenizing the datasets from the model simulations.

APPENDIX

Sensitivity to Models' Region of Maximum Rainfall Variability

The region of maximum precipitation variability as defined by observations (Fig. 2a) has been used to study simulated precipitation variability over the very same region in the warm-season months. However, this region is not necessarily the region of maximum pre-

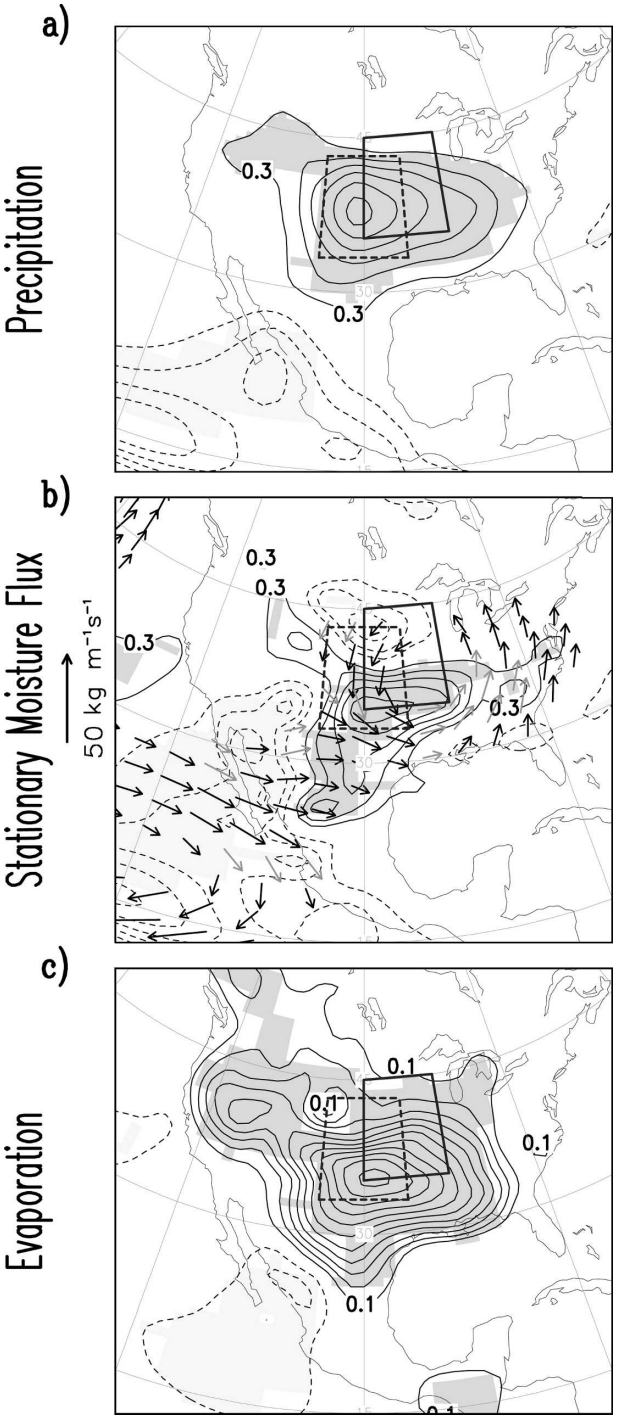

FIG. A1. Warm-season regressions of a shifted GPP index on (a) precipitation, (b) stationary moisture fluxes, and (c) evaporation anomalies from the GFDL-CM2.1 simulation. This shifted index is defined along the maximum of standard deviation in the GFDL-CM2.1 simulation (Fig. 2c, dashed line box), and noted in this figure by the enclosed dashed box. The index is displaced southwestward with respect to the region of maximum observed in NARR (noted here as the continuous line box). As in previous figures precipitation and moisture flux convergence are contoured with the same 0.3 mm day^{-1} interval, and evaporation with a 0.1 mm day^{-1} interval; dark (light) shading denotes areas of positive (negative) anomalies as in Figs. 5–7.

cipitation variability in simulations (Figs. 2b–g), which opens the question about the generality of the results. To address this issue, and as an example, the analysis is repeated for the GFDL-CM2.1 model whose westward shift of the region of maximum precipitation variability (as compared with observations) is typical of the simulations. The region of maximum precipitation variability of this model can also be enclosed in a 10° latitude–longitude box (Fig. 2c, dashed box: 33°–43°N, 105°–95°W), as the original definition of the Great Plains region. The precipitation index is generated from area-averaged precipitation anomalies over this shifted box of maximum precipitation variability during the warm-season months. Then it is regressed onto precipitation, moisture fluxes, and evaporation anomalies.

The new index does not improve the structure of anomalies associated to the precipitation variability of the region. As expected, the regressed precipitation anomalies (Fig. A1a) are centered over the region of definition of the index and are larger than those with the original GPP index (Fig. 5c). The regressed vertically integrated moisture flux anomalies and their convergence (Fig. A1b) are also larger than before (Fig. 6c); the artificial link with the Pacific basin via moisture fluxes is even stronger than it was before, and the connection with the Gulf of Mexico is still absent. Evaporation anomalies (Fig. A1c) remain of the same magnitude as before (Fig. 7c). It is also clear that according to this displaced region, maximum anomalies are more centered over the region than they were over the Great Plains region.

The relative importance of the water balance components over the shifted region does not change or the significance of precipitation recycling via local evaporation. In the mean, area-averaged anomalies are larger than before: mean precipitation increases from 1.13 to 1.28 mm day^{-1}, mean moisture flux convergence increases from 0.40 to 0.50 mm day^{-1}, and evaporation increases from 0.59 to 0.67 mm day^{-1}. This picture of a larger control by land surface processes on precipitation variability is further corroborated by obtaining the autocorrelation of the shifted index (as it was done before for the GPP index; Fig. 8). Now, the dependence of July's precipitation on previous months' precipitation is larger than before, with correlations of 0.5 for May, and 0.8 for June.

Thus, it is apparent that focusing on the individual regions of maximum precipitation variability of the different models, in contrast to the region identified by observations, does not change the main results of the present study but further strengthens them.

REFERENCES

Delworth, T. L., and Coauthors, 2006: GFDL's CM2 global coupled climate models. Part I: Formulation and simulation characteristics. *J. Climate,* **19,** 643–674.

Gordon, C., C. Cooper, C. A. Senior, H. Banks, J. M. Gregory, T. C. Johns, J. F. B. Mitchell, and R. A. Wood, 2000: The simulation of SST, sea ice extents and ocean heat transports in a version of the Hadley Centre coupled model without flux adjustments. *Climate Dyn.,* **16,** 147–168.

Hasumi, H., and S. Emori, Eds., 2004: K-1 coupled GCM (MIROC) description. K-1 Tech. Rep. 1, 39 pp. [Available online at http://www.ccsr.u-tokyo.ac.jp/kyosei/hasumi/MIROC/tech-repo.pdf.]

Kalnay, E., and Coauthors, 1996: The NCEP/NCAR 40-Year Reanalysis Project. *Bull. Amer. Meteor. Soc.,* **77,** 437–471.

Koster, R., and Coauthors, 2004: Regions of strong coupling between soil moisture and precipitation. *Science,* **305,** 1138–1140.

——, and Coauthors, 2006: GLACE: The Global Land–Atmosphere Coupling Experiment. Part I: Overview. *J. Hydrometeor.,* **7,** 590–610.

Meehl, G. A., W. M. Washington, C. Ammann, J. M. Arblaster, T. M. L. Wigley, and C. Tebaldi, 2004: Combinations of natural and anthropogenic forcings and twentieth-century climate. *J. Climate,* **17,** 3721–3727.

Mesinger, F., and Coauthors, 2004: NCEP North American regional reanalysis. Preprints, *15th Symp. on Global Change and Climate Variations,* Seattle, WA, Amer. Meteor. Soc., CD-ROM, P1.1.

Mitchell, K., and Coauthors, 2004: NCEP completes 25-year North American Reanalysis: Precipitation assimilation and land surface are two hallmarks. *GEWEX Newsletter,* No. 14, International GEWEX Project Office, 9–12.

Nigam, S., and A. Ruiz-Barradas, 2006: Seasonal hydroclimate variability over North America in global and regional reanalyses and AMIP simulations: Varied representation. *J. Climate,* **19,** 815–837.

Pope, V. D., M. L. Gallani, P. R. Rowntree, and R. A. Stratton, 2000: The impact of new physical parametrizations in the Hadley Centre climate model–HadAM3. *Climate Dyn.,* **16,** 123–146.

Ruiz-Barradas, A., and S. Nigam, 2005: Warm-season precipitation variability over the U.S. Great Plains in observations, NCEP and ERA-40 reanalyses, and NCAR and NASA atmospheric simulations. *J. Climate,* **18,** 1808–1830.

——, and S. Nigam, 2006: Great Plains hydroclimate variability: The view from North American regional reanalysis. *J. Climate,* **19,** 3004–3010.

Schmidt, G. A., and Coauthors, 2006: Present-day atmospheric simulations using GISS ModelE: Comparison to in situ, satellite, and reanalysis data. *J. Climate,* **19,** 153–192.

Wu, W., and R. E. Dickinson, 2005: Warm-season rainfall variability over the U.S. Great Plains and its correlation with evapotranspiration in a climate simulation. *Geophys. Res. Lett.,* **32,** L17402, doi:10.1029/2005GL023422.